Frontiers in Bioscience Landmark

Front. Biosci. (Landmark Ed) **2025**; 30(8): 41226
https://doi.org/10.31083/FBL41226

Original Research

LONP1 Promotes Hepatocarcinogenesis by Degrading ACO2 to Alleviate Ferroptosis

Yanfeng Zhong[1,†], Liusheng Wu[2,†], Zhen Peng[3], Wei Mao[4], Ting Wang[3], Bo Wu[3], Zhendong Yu[5], Xiaoqiang Li[6,*], Erbao Chen[3,*]

[1]Central Laboratory, Peking University Shenzhen Hospital, 518036 Shenzhen, Guangdong, China
[2]Yong Loo Lin School of Medicine, National University of Singapore, 119077 Singapore, Singapore
[3]Department of Hepatobiliary and Pancreatic Surgery, Peking University Shenzhen Hospital, 518036 Shenzhen, Guangdong, China
[4]Department of Oncology, Shenzhen Key Laboratory of Gastrointestinal Cancer Translational Research, Cancer Institute, Peking University Shenzhen Hospital, Shenzhen Peking University-Hong Kong University of Science & Technology Medical Center, 518036 Shenzhen, Guangdong, China
[5]Blood Transfusion Department, Peking University Shenzhen Hospital, 518036 Shenzhen, Guangdong, China
[6]Department of Thoracic Surgery, Peking University Shenzhen Hospital, 518036 Shenzhen, Guangdong, China
*Correspondence: dr.lixiaoqiang@gmail.com (Xiaoqiang Li); ebchen17@fudan.edu.cn (Erbao Chen)
[†]These authors contributed equally.

Academic Editor: Sung Eun Kim
Submitted: 14 May 2025 Revised: 26 July 2025 Accepted: 5 August 2025 Published: 29 August 2025

Abstract

Background: Lon protease 1 (LONP1), an adenosine triphosphate (ATP)-dependent protease encoded by nuclear DNA that is highly conserved, maintains the mitochondrial protein balance and regulates adaptive responses to cellular stress. LONP1 dysfunction ultimately results in various forms of cellular and tissue damage. The function of LONP1 in hepatocellular carcinoma (HCC) and how it affects HCC growth were investigated in this work. **Methods**: The RNA and protein expression levels of LONP1 were determined in paired HCC and adjacent tissue samples through real-time quantitative polymerase chain reaction (RT-qPCR) and immunohistochemistry (IHC) staining. The correlation between LONP1 expression and clinical features was evaluated via statistical analysis. Overexpression (OE) and knockdown (KD) experiments, small RNA interference, Cell Counting Kit-8 (CCK8) and wound-healing assays, and animal experiments were employed to assess the potential mechanism by which LONP1 promotes the proliferation and migration of HCC cells both *in vitro* and *in vivo*. **Results**: In HCC samples, LONP1 expression was higher than in the equivalent surrounding tissues. Compared to patients with low LONP1 expression, individuals with high LONP1 expression had shorter disease-free survival and overall survival periods. Functionally, LONP1 facilitated the proliferation and migration of HCC cells, whereas LONP1 knockdown mitigated the growth of HCC subcutaneous tumors. Mechanistically, LONP1 affects the processes of ferroptosis and cuproptosis processes by regulating the stability of aconitase 2 (ACO2). Histological analysis showed that the expression of LONP1 in liver cancer tissues was significantly upregulated, accompanied by a decrease in the level of ACO2 protein (Hematoxylin-Eosin (HE) staining and IHC verification). Mitochondrial function experiments indicated that overexpression of LONP1 led to a significant decrease in mitochondrial membrane potential suggesting mitochondrial dysfunction and reduced susceptibility to ferroptosis. **Conclusions**: Our results suggest that LONP1 promotes HCC proliferation and migration by inhibiting ferroptosis and cuproptosis through the degradation of ACO2. Therefore, targeting LONP1 might be an effective therapeutic strategy to inhibit HCC growth.

Keywords: Lon protease 1 (LONP1); hepatocellular carcinoma; ferroptosis regulation; aconitase 2 (ACO2); survival prognosis

1. Introduction

Since it makes up 90% of primary liver malignancies, hepatocellular carcinoma (HCC) is the most common histological subtype of liver cancer and has a high death rate. It ranks as the third most frequent cause of cancer-related mortality globally [1], and is especially common in Asia, Africa and southern Europe [2]. HCC is known as the "king of cancers" because of its biological characteristics, such as high malignancy, strong invasiveness and easy metastasis. The main occurrence factors of HCC include genetic and epigenetic changes, chronic hepatitis B virus or hepatitis C virus exposure, aflatoxin exposure, smoking, obesity and diabetes [1,3]. The incidence of HCC associated with metabolic dysfunction-associated fatty liver disease (MAFLD) is increasing in Western countries [4], and the high recurrence and metastasis rates of HCC lead to serious adverse prognoses [5]. Although patients with HCC have a wide range of treatment options, including liver transplantation, surgical resection, percutaneous ablation and radiotherapy, as well as standard treatment methods such as transarterial and systemic therapy [6], more than 70% of advanced cases are not suitable for transplantation or surgery [7]. Current studies on the dysregulation of key signaling pathways, epigenetic modifications, and the tumor microenvironment in HCC progression have provided novel insights for intervention strategies [8–10]. However, the current understanding of the molecular mechanisms un-

derlying HCC progression and metastasis remains incomplete. In-depth investigation of its pathological mechanisms is crucial for identifying early biomarkers and improving treatment approaches.

Lon protease 1 (LONP1) is a highly conserved adenosine triphosphate (ATP)-dependent protease encoded by nuclear DNA and located in the mitochondrial matrix. This protein mediates the selective degradation of misfolded or oxidation-damaged polypeptides in the mitochondrial matrix, maintains the mitochondrial protein balance and regulates adaptive responses to cellular stress [11,12]. Mitochondrial dysfunction is a signature phenomenon in cancer biology and may be one of the reasons for the transformation of mitochondrial energy metabolism in tumor tissues from aerobic respiration to glycolysis, a process that requires less oxygen. Dysfunction of LONP1 directly leads to the failure of mitochondrial protein degradation, and the accumulation of abnormal mitochondrial proteins leads to a series of types of cells and tissue damage. Previous studies have shown that the upregulation of LONP1 helps lung fibroblasts adapt to acute stress and is important for maintaining normal cell viability [13] and overcoming hypoxia and metabolic and proteotoxic stress associated with the oncogenic transformation of tumor cells [14]. Silencing LONP1 leads to apoptosis and mitochondrial damage in colon cancer cells, and LONP1 is involved in epithelial–mesenchymal transition (EMT) in colon cancer cells [15]. It has shown that some long non-coding RNAs (lncRNAs) impair CD4+ T-cell activation by targeting LONP1, leading to a poor prognosis in patients with gastric cancer [16]. *Helicobacter pylori* partially induce LONP1 expression and overgrowth of gastric cancer cells through HIF1α regulation [17].

An iron-dependent type of regulatory cell death linked to an excessive buildup of lipid peroxides is known as ferroptosis [18,19], and limiting cytotoxic lipid peroxidation protects cells against ferroptosis. Current studies on the mechanism of ferroptosis have confirmed that inhibiting the activity of System Xc^- and glutathione peroxidase 4 (GPX4) can induce ferroptosis, which is inhibited by erastin and RSL3, respectively [20,21]. GPX4 is the main enzyme that catalyzes the neutralization of phospholipid hydroperoxides (PLOOH) in mammalian cells, peroxidation of lipid hydrogen and reduction to the corresponding alcohol. *GPX4* gene deletion is known to cause lipid peroxidation-dependent cell death in mouse embryonic fibroblasts [22], and uncontrolled lipid peroxidation is a marker of ferroptosis. Acyl-coa synthase long chain family member 4 (ACSL4) is an important driver of ferroptosis [23,24] and is regulated by multiple signaling pathways [25, 26]. The expression of ACSL4 in the triple-negative breast cancer cell line subpopulation is related to its sensitivity to ferroptosis inducers [23], and this correlation also exists in clear cell renal cancer cells [24]. p53 may promote ferroptosis by inhibiting the transcription of solute carrier family 7 member 11 (SLC7A11), the subunit of System Xc^-, and thus exerting its tumor suppressor function [27]. Arachidonate 12-lipoxygenase (ALOX12) has been reported to be essential for tumor protein 53 (p53)-dependent ferroptosis induced by peroxide [28]. It has reported that PE binding protein-1 (PEBP1) can interact with some lipoxygenases (LOXs) and participate in the regulation of ferroptosis [29]. The protein encoded by the aconitase 2 (*ACO2*) gene belongs to the cis-aconitase/isopropylmalate (IPM) isomerase family. This protein, which is encoded in the nucleus and plays a role in mitochondria, is a mitochondrial matrix protein that catalyzes the mutual conversion of citric acid to isocitric acid through cisaconite acid in the second step of the tricarboxylic acid cycle (TCA). It is involved mainly in the anabolism and catabolism of organisms, such as DNA repair and replication, as well as protein synthesis and degradation, and its expression products are widely distributed in the heart, kidney and other tissues and organs. Studies have shown that pathogenic gene variation or disordered expression of ACO2 is involved in neurodegenerative syndromes such as optic neuropathy [30] and Parkinson's disease [31]. Abnormal expression of the Fe-S cluster protein ACO2 leads to mitochondrial dysfunction, and abdominal aortic aneurysm [32]. In addition, mitochondrial dysfunction leads to metabolic changes and affects the activation process of macrophages [33].

Ferroptosis is closely related to HCC development, but its mechanism of action remains unclear [34,35]. Our study revealed that silencing LONP1 leads to the accumulation of malondialdehyde (MDA) and reactive oxygen species (ROS) in liver cancer cells, suggesting that abnormal LONP1 expression is associated with ferroptosis in these cells. However, the role of LONP1 in iron-related death in liver cancer is unknown. In this project, the expression, biological function and mechanism of LONP1 were studied in the field of HCC. These findings help to elucidate the new mechanism of HCC development and metastasis, provide new ideas for the treatment and diagnosis of HCC, and may also provide important reference value for similar studies of other tumors or diseases.

2. Materials and Methods

2.1 Data Processing

HCC sequence data and related clinicopathological data were extracted from The Cancer Genome Atlas (TCGA, https://portal.gdc.cancer.gov/) and compiled from the TCGA database using RNAseq data from 33 tumor projects processed using the spliced transcripts alignment to a reference (STAR) process and data in TPM (transcripts per million reads) format. There were 424 tumor samples and 50 normal samples collected (duplicate samples were eliminated, but clinical data was kept). Paracancer and cancer samples that matched the correct numbers were also extracted. For the purpose of comparing expression across samples, the RNA-seq data in TPM format were trans-

formed to log2(value + 1) values. The Stats [4.2.1, https://cran.r-project.org/bin/windows/base/old/4.2.1/] R software package and car package [3.1-0] were used to select appropriate statistical methods according to the data format characteristics (statistical analysis was not performed if the statistical requirements were not met), and the ggplot2 package [3.3.6, https://cran.r-project.org/src/contrib/Archive/ggplot2/] was used to visualize the data.

Since the TCGA database is open to the public according to specific guidelines, it confirms that written informed consent was obtained from all the subjects prior to data collection.

2.2 Identification and Functional Enrichment of Differentially Expressed Genes (DEGs) in HCC

A total of 424 HCC patients were divided into high and low LONP1 expression groups according to the median LONP1 expression. The R package DESeq2 [1.36.0, https://mghp.osn.xsede.org/bir190004-bucket01/index.html#archive.bioconductor.org/packages/3.15/bioc/src/contrib/DESeq2] was used to identify intergroup DEGs. The clusterProfiler [4.4.4, https://mghp.osn.xsede.org/bir190004-bucket01/index.html#archive.bioconductor.org/packages/3.15/bioc/src/contrib/clusterProfiler] and GOplot [1.0.2, https://cran.r-project.org/web/packages/GOplot/] R packages were subsequently used to conduct Gene Ontology/Kyoto Encyclopedia of Genes and Genomes (GO/KEGG) combined LogFC enrichment analysis for the identified DEGs, and the org.Hs.eg.db package [3.21.0, https://bioconductor.org/packages/release/data/annotation/html/org.Hs.eg.db.html] was subsequently used to convert the Entrez ID for the input DEGs. The clusterProfiler package [4.4.4] is used for enrichment analysis, and the LogFC value of DEGs is used to calculate the corresponding z score value of each enrichment item through the GOplot package to preliminarily determine whether the corresponding item is positively regulated (z score is positive) or negatively regulated (z score is negative). The enrichment analysis results were visualized via the ggplot2 package.

$$\text{zscore} = \frac{(UP - DOWN)}{\sqrt{\text{counts}}}$$

2.3 Analysis of the Clinical Significance of LONP1 Expression in HCC

In order to provide light on the clinical relevance of LONP1 expression, we examined how LONP1 expression varied during the course of the disease (stage I, stage II, stage III, and stage IV). The statistical methods used are the global test (Kruskal–Wallis test) and the multiple hypothesis test (Dunn's test). The effectiveness of the LONP1 expression level in differentiating HCC tissues from nontumor tissues was compared via receiver operating characteristic (ROC) curve analysis to test its predictive value in HCC diagnosis. Three prognostic indices, overall survival (OS), disease-specific survival (DSS) and the progression-free interval (PFI), were evaluated. A survival kit was subsequently used to conduct a proportional risk hypothesis test and univariate and multivariate Cox regression analyses to analyze the possibility that LONP1 is an independent risk factor for HCC. The risk factors for Cox regression were $p < 0.05$.

2.4 Cell Culture and Transfection

The Huh7 cell lines were purchased from the Guangzhou Cellcook Biotech Co., Ltd (Guangdong, China). Dulbecco's Modified Eagle Medium (DMEM, Invitrogen, CA, USA) containing 10% Fetal Bovine Serum (FBS, Gibco, CA, USA) and 1% penicillin and streptomycin double antibody was used to culture Huh7 cells in an incubator at 37 °C and 5% CO_2. All cell lines were validated by STR profiling and tested negative for mycoplasma. After logarithmic growth, siLONP1 (SIGS0001490-1, RiboBio, Guangzhou, China, 5′-ACCACTCCTCGGAGTTCAA-3′) and siNC (RiboBio, Guangzhou, China, siNC0000001-1-5) were transferred into Huh7 cells via Lipofectamine™ 3000 (Invitrogen, Carlsbad, CA, USA, L3000015). The cells were divided into the siLONP1 group and the siNC group. The cell plates were placed in incubators for further culture. After transfection for 48 h, RNA was collected for real-time quantitative polymerase chain reaction (RT-qPCR) detection, and protein samples were collected for Western blot detection.

2.5 Lentivirus Infection of Huh7 Cells

The Huh7 cells were counted and put onto 6-well cell culture plates following digestion. The plates were then incubated with a 5% CO_2 volume fraction at 37 °C for the entire night. A total of 30~40% of the cells were infected with lentivirus (shRNA targeting LONP1: 5′-CCGGGCAAGATCCTCTGCTTCTATGCTCGAGCATAGAAGCAGAGGATCTTGCTTTTTG-3′). The medium was changed to fresh medium 12 hours after virus infection, and the cells were collected 48 hours after the medium was changed for subsequent detection.

2.6 RT-qPCR

A total of 144 HCC cancer tissues and corresponding adjacent non-tumor samples were collected from patients who received curative hepatectomies between January 2015 and December 2018 at Peking University Shenzhen Hospital, and were constructed into tissue microarrays (TMA).

Another cohort of 71 fresh HCC sample pairs was obtained from HCC patients undergoing curative resection between January 2020 and December 2020 at the Department of Hepatobiliary and Pancreatic Surgery. Thus, a total of 215 clinical sample were involved in the study. TRIzol was used to grind RNA from hepatocellular carcinoma

Table 1. Primers for qRT-PCR.

Primer ID	Primer sequences (5′–3′)
LONP1 - forward	TATGGAGATGATCAACGTGTCG
LONP1 - reverse	GACAATCTTGTAGGCCGATTTC
β-actin - forward	AAAGACCTGTACGCCAACAC
β-actin - reverse	GTCATACTCCTGCTTGCTGAT
ACO2 - forward	GCAACGACGCAAACCCC
ACO2 - reverse	CCATCCCACTTGTCAAAAGGCT
ATP7A - forward	TGGTGGGTACAGGAGTAGGTGC
ATP7A - reverse	GGGGTTCCGTGAGTAATGGTTC
ATP7B - forward	GGGGTTCAAAGTATTCAAGTGTCC
ATP7B - reverse	GGCAATGGCAATCAGAGTGGT
DLAT - forward	CTGCTGCCACTGCTTCGC
DLAT - reverse	TCCTTCACTTAGCTTCTCACCCA
FAM50A - forward	ATCGAGACCGTGAGGAGGAG
FAM50A - reverse	TTTCCGAAGGATCTCGAGCG
FDX1 - forward	ACCCTGGCTTGTTCAACCTGT
FDX1 - reverse	TGGCAGCCCAACCGTGA
HSPA4 - forward	GTACTGTGGACCTGCCAATCG
HSPA4 - reverse	AGCATCATTCCGCTCCTTCTC
LIAS - forward	GATGCCAGTGAGCCCTACAAT
LIAS - reverse	CCCCATCAGGCATATCATCTCG
PUS1 - forward	GCGGGTTTAACTCCAAGAACAG
PUS1 - reverse	GCTCAGGCGGTAGGTCTCAT
SLC31A1 - forward	ACAATTCCATGCCTGTCCCA
SLC31A1 - reverse	TCCACTACCACTGCCTTCTTC

tissues and paired normal or paracancerous tissues, and a NanoDrop 2000 (Thermo Fisher Scientific, Waltham, MA, USA) was used to determine the RNA concentration. The RNA samples whose D260 nm/D280 nm ratio ranged from 1.9 to 2.1 were retained. A RT kit (R323-01, Vazyme, Nanjing, China) was used for reverse transcription with 1 µg of RNA. SYBR Green Real-time PCR Master Mix (Q121-02, Vazyme, Nanjing, China) and a Roche LightCycler 480 Real-Time PCR system (Roche Diagnostics, Basel, Switzerland) were used for the relative quantitative analysis of genes expression level. Details of the qPCR primer sequences are presented in Table 1. The data were analyzed via the $2^{-\Delta\Delta CT}$ method.

2.7 Western Blots

Cells were lysed and their proteins extracted using radio immunoprecipitation assay (RIPA) buffer (Beyotime, Shanghai, China, P0013B) containing 1 mM phenylmethanesulfonyl fluoride (PMSF, Beyotime, Shanghai, China, ST506) and a protease inhibitor combination (Beyotime, Shanghai, China, P1005). After protein transfer, the polyvinylidene fluoride (PVDF) membrane (Millipore, Burlington, MA, USA, IPVH00010) was placed in 3% bovine serum albumin (BSA, Sangon, Shanghai, China, A600332) and incubated at room temperature for 1 h. An enhanced chemiluminescence (ECL) substrate (Biosharp, Beijing, China, BL520A) was added, and the signal was detected via a chemiluminescence imaging and analysis system (Cytiva, Uppsala, Sweden, GE AI800). Anti-LONP1 antibody (Proteintech, Chicago, IL, USA, 15440-1-AP, 1:1000), anti-beta-actin antibody (Proteintech, Chicago, IL, USA, 66009-1-Ig, 1:500), anti-ACO2 antibody (Proteintech, Chicago, IL, 11134-1-AP, 1:1000), horseradish peroxidase (HRP)-coupled goat anti-mouse antibody (ABclonal, Wuhan, China, AS003, 1:500), and HRP-coupled goat anti-rabbit antibody (ABclonal, Wuhan, China, AS014, 1:500) were used.

2.8 Cell Proliferation Experiment

Negative control (NC) cells and cells overexpressing LONP1 (LONP1-OE) were trypsinized, tallied, and seeded onto 96-well plates at a density of 2000 cells per well. Four replicates per group were cultivated for 0, 24, 48, 72, 96 hours in a 37 °C CO_2 incubator. Each well was then filled with 10 µL of CCK8 solution (Solarbio, Beijing, China, CA1210), and the wells were incubated for an additional hour. A microplate reader (Thermo Fisher Scientific, MA, USA, MultiskanGO) was used to measure absorbance at 450 nm. Cells with LONP1 knockdown (LONP1-KD) and their respective negative control group (shRNA) were processed identically.

2.9 Migration Assay

Approximately 5×10^5 cells were inoculated into a 6-well plate. After the cells were attached to the wall and

the confluence reached 100%, a scratch operation was performed. Then, the cells were washed with PBS 3 times, the scratched cells were removed, and fresh media without serum was added. The samples were then placed back into a 5% CO_2 incubator at 37 °C and photographed again under a microscope (Leica, Wetzlar, Germany, DMI8) at 24 h. Twenty-four-hour mobility = (0 h scratch width – 24 h scratch width)/0 h scratch width × 100%.

2.10 Immunohistochemistry

Paraffin sections were processed via the UltraSensitive™ SP (Mouse/Rabbit) IHC Kit (MXB Biotechnologies, Fuzhou, China, KIT-9720) according to the laboratory instructions. The paraffin-embedded sections were incubated overnight at 4 °C with a specified dilution of antibody. DAB color development reagent (ZSGB-BIO, Beijing, China, ZLI-9017) was used, and the samples were sealed with neutral resin (Biosharp, BL704A). Anti-LONP1 antibody (Proteintech, Chicago, IL, 15440-1-AP, 1:200) and anti-ACO2 antibody (Proteintech, Chicago, IL, 11134-1-AP, 1:1000) were used.

2.11 Subcutaneous Tumor Model in Nude Mice

Huh7-shNC and LONP1-KD stable transfer cell lines were digested with pancreatic enzymes, the washed cells were precooled with PBS 3 times and counted, and the cells were injected into the subcutaneous area of the armpits of nude mice according to the number of cells at the site 5×10^6. Two weeks later, the tumor size and weight were measured and photographed.

The male BALB/c-nu mice (4 weeks old) used in the experiment were purchased from Weitonglihua (Beijing, China) Biotechnology Co., Ltd. All mice were raised in a specific pathogen-free (SPF) grade barrier environment at the Laboratory Animal Center of Peking University - Hong Kong University of Science and Technology Medical Center. The environmental conditions were: temperature 22 ± 2 °C, relative humidity 50 ± 10%, and 12 hours of light/dark cycling. Mice can freely obtain standard rodent feed and sterilized drinking water. All animal experiments and operations strictly adhere to the experimental protocols approved by the Laboratory Animal Ethics Committee of Peking University Shenzhen Hospital, as well as national and international laboratory animal welfare guidelines.

2.12 Statistical Analysis

Post-hoc multiple comparisons were conducted using Dunn's test, which is appropriate for non-normally distributed data. Pairwise comparisons were performed to identify which specific groups exhibited statistically significant differences. For survival analysis, the Kaplan-Meier (KM) method was employed, with the Log-Rank test used to determine the *p*-value. All cellular experiments were replicated to ensure reliability. Data from these experiments were analyzed using the *t*-test, with results presented as mean ± standard deviation (mean ± SD). A *p*-value less than 0.05 was considered indicative of statistical significance.

3. Results

3.1 Abnormal Expression of LONP1 in Hepatocellular Carcinoma

The expression of LONP1 mRNA in various tumor types was examined using the Wilcoxon rank sum test based on the TCGA data (Fig. 1A). Compared with that in normal tissues, LONP1 was differentially expressed in 17 types of tumors, such as bladder urothelial carcinoma (BLCA) and breast invasive carcinoma (BRCA) ($p < 0.01$). In addition, we used a multicancer microarray to verify that the LONP1 protein was highly expressed in multiple tumor types (Fig. 1B). LONP1 was significantly overexpressed in unmatched HCC samples ($p < 0.001$). In addition, a comparative analysis of liver cancer tissue samples from 50 pairs of patients in the TCGA-HCC dataset and their paired normal liver tissue samples revealed that LONP1 was significantly overexpressed in HCC tissues (Fig. 1C). On the basis of the results obtained from the above biological information database analysis, we collected clinical samples of cancer tissues and adjacent tissues from HCC patients to detect LONP1 mRNA expression in HCC. The RT-qPCR results of 71 cancer and paracancerous tissues revealed that LONP1 was significantly overexpressed in the cancer tissues of HCC patients (Fig. 1D). To further verify the expression of the LONP1 proteins, 144 liver cancer tissue samples were subjected to immunohistochemical staining. The results revealed that the expression of LONP1 in cancer tissue was significantly greater than that in paracancerous tissue (Fig. 1E,F).

To explore the reference value of the LONP1 expression level in distinguishing HCC samples from normal samples, ROC curve analysis was first performed on RNA-seq samples in the TCGA database (Fig. 1G), and the results revealed that the area under roc curve (AUC) value of LONP1 was 0.863 (95% CI: 0.820–0.906), suggesting that LONP1 could be used as a diagnostic marker for HCC but was not associated with tumor stage (Fig. 1H). To further clarify whether differences in LONP1 expression are associated with poor prognosis in HCC patients, we analyzed the clinical information of 370 HCC RNAseq samples in the TCGA database. LONP1 expression was divided into high and low-expression groups according to the median value of LONP1 expression. K–M survival analysis revealed that LONP1 was associated with OS (Fig. 1I) but was not a risk factor for the PFI or DSS of patients with HCC (Fig. 1J,K).

3.2 LONP1 Regulates Huh7 Cell Proliferation and Migration and Tumor Growth

To further elucidate the biological function and mechanism of LONP1 and screen suitable liver cancer cell lines

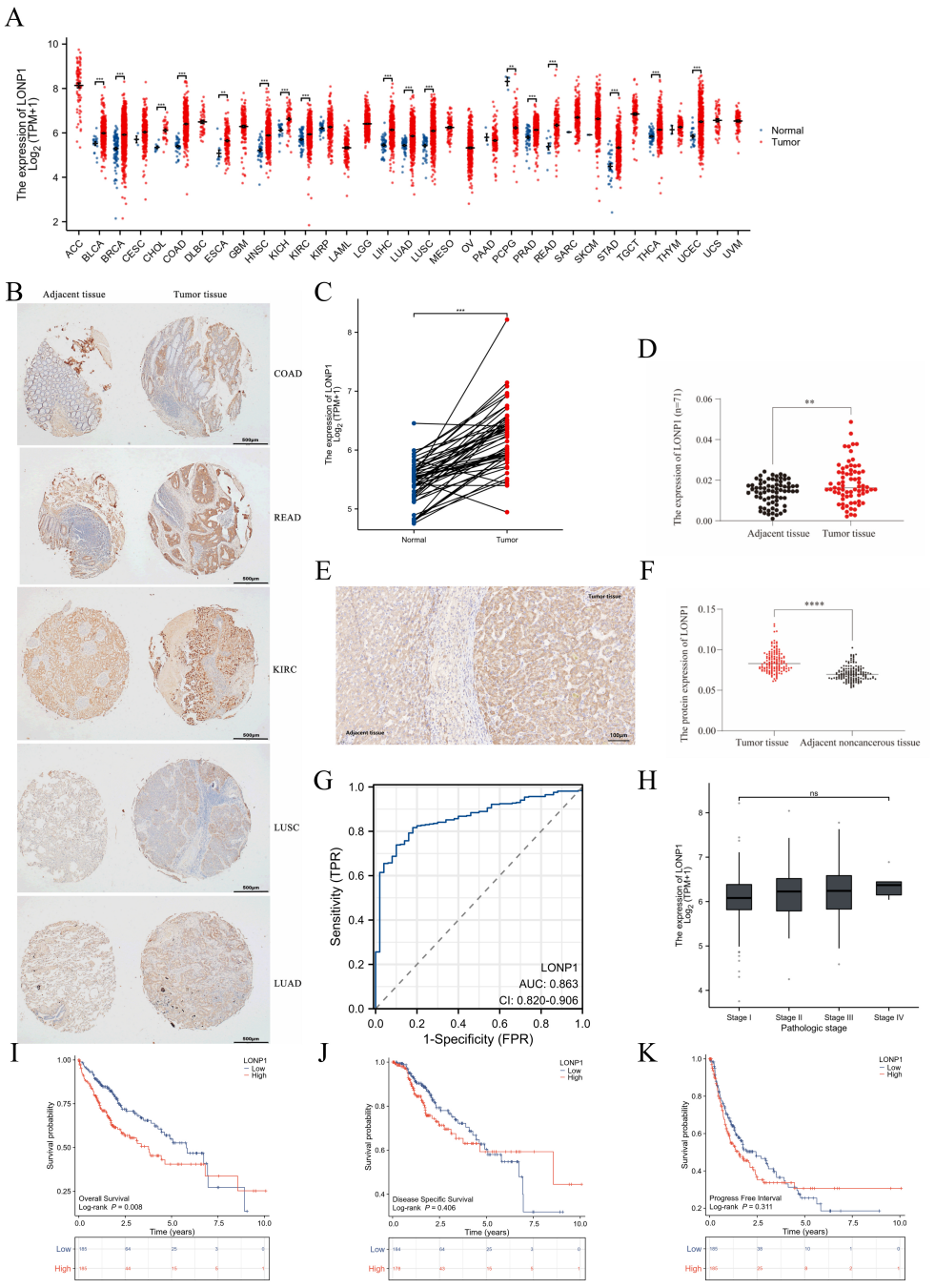

Fig. 1. Expression characteristics of LONP1 (LONP1 RNA level increased, diagnostic and prognostic value). (A) Expression of LONP1 in 11,123 unmatched cancer-associated RNAseq samples. (B) The IHC statinging of a pancancer chip indicated that LONP1 is highly expressed in a variety of tumors. Scale bar = 500 μm. (C) Expression of LONP1 in 50 paired HCC samples. (D) LONP1 expression in 71 paired hepatocellular carcinoma- and paracarcinoma-related mRNA samples. (E) IHC staining was used to detect the expression of LONP1 in liver cancer tissues, and representative image was showed. Scale bar = 100 μm. (F) LONP1 protein expression levels in 144 liver cancer microtissue chips were scored on the basis of the average optical density value. (G) ROC curve analysis of the correlation of differences in LONP1 expression with HCC diagnosis. (H) Correlation between LONP1 expression and the tumor stage of HCC. (I–K) KM curves were used to analyze the correlations between high and low LONP1 expression in patients with liver cancer in terms of OS, PFI, DSS and other clinical indicators. The data used for the analysis were derived from the RNAseq data platform in the TCGA database. LONP1, Lon protease 1; IHC, immunohistochemistry; HCC, hepatocellular carcinoma; ROC, receiver operating characteristic; KM, Kaplan-Meier; OS, overall survival; PFI, progression-free interval; DSS, disease-specific survival; TCGA, The Cancer Genome Atlas. $^{**}p < 0.01$; $^{***}p < 0.001$; $^{****}p < 0.0001$; ns, not significant.

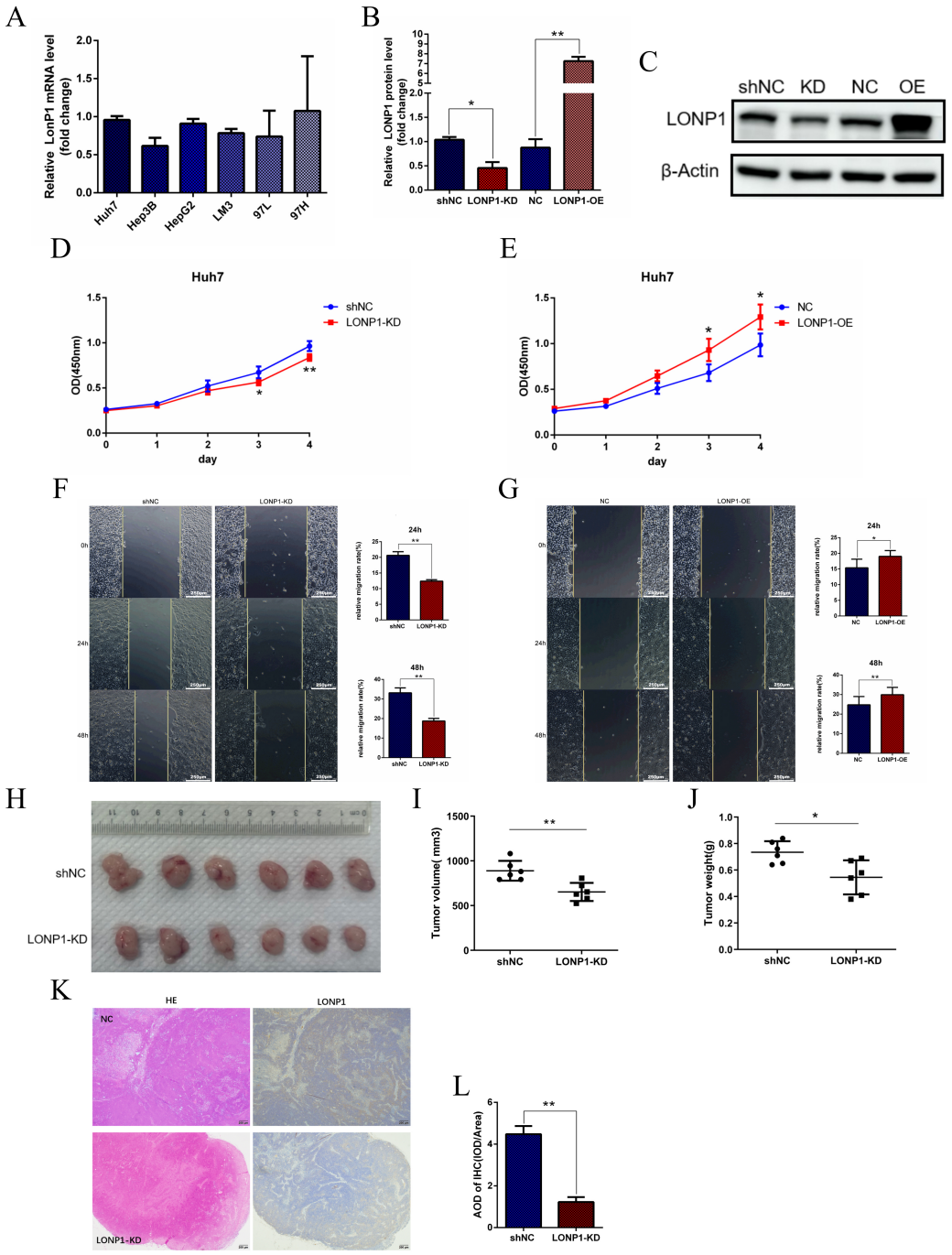

Fig. 2. LONP1 expression regulates cell proliferation, migration and tumor formation. (A) RT-qPCR was used to detect the expression of LONP1 in the mRNA samples of various hepatoma cell lines. (B,C) After lentivirus infection of Huh7 cells, stable knockdown and overexpression cell lines were constructed, and the relative expression of LONP1 was detected via western blotting. The internal reference was beta-actin, and representative images were showed. (D,E) CCK8 was used to detect the activity of Huh7 cells with LONP1 knockdown or overexpression. (F,G) The migration ability of Huh7 cells with low knockdown or overexpression of LONP1 was detected via a wound healing assay. Scale bar = 250 µm. (H–J) Huh7 stable cells with LONP1 knockdown were inoculated into subcutaneous tumors formed at the lateral axilla of nude mice, and the number of cells inoculated at each site was 5×10^6. (K,L) Hematoxylin-Eosinand Immunohistochemistry of Liver cancer subcutaneous tumors section. The results of the Western blot and wound healing experiments were analyzed via ImageJ software (an open-source Java-based image processing program developed by the National Institutes of Health). Scale bar = 200 µm. The data are expressed as the means ± SDs of at least three independent experiments. KD, knockdown; NC, negative control; OE, overexpression; HE, hematoxylin-eosin staining. *$p < 0.05$, **$p < 0.01$.

for further study, we analyzed the expression of the *LONP1* gene in a variety of liver cancer cell lines (Fig. 2A) and finally selected the Huh7 cell line with stable expression of LONP1 as the object of subsequent functional and mechanistic studies.

In this study, lentivirus interference was used to inhibit and overexpress LONP1 in Huh7 cells, and its inhibitory and overexpression effects were verified at the mRNA and protein levels (Fig. 2B,C). Next, we detected cell viability after the inhibition or overexpression of LONP1 via a CCK8 assay. The results showed that the inhibition of LONP1 expression decreased the activity of Huh7 cells, whereas the overexpression of LONP1 increased activity of Huh7 cells (Fig. 2D,E), suggesting that LONP1 is involved in regulating the proliferation of Huh7 cells. Subsequently, wound healing assays were used to determine whether the migration capacity of the cells was affected by LONP1. Compared with the control, inhibition of LONP1 expression significantly reduced the mobility of Huh7 cells, whereas overexpression of LONP1 promoted migration (Fig. 2F,G), indicating that LONP1 expression regulated the migration ability of Huh7 cells. To further clarify the function of LONP1, we derived a stable Huh7 cell line derived from LONP1 via lentivirus and inoculated it subcutaneously into 4-week-old nude mice to construct a CDX model. The tumor samples were extracted, measured and weighed two weeks later. According to the results, the experimental group with reduced LONP1 expression had smaller tumors in terms of both weight and volume than the control group (Fig. 2H–J), and LONP1 in liver cancer tissues was significantly upregulated (Fig. 2K,L), indicating that inhibiting LONP expression could inhibit the formation of transplanted Huh7 tumors.

3.3 LONP1 Affects the Tumor Microenvironment and is Involved in the Regulation of Iron-induced Cell Death

To explore the potential biological function of the *LONP1* gene differentially expressed in HCC, a total of 681 genes were significantly differentially expressed in the *LONP1* gene ($|\text{LogFC}| \geq 1$, $p.\text{adj} < 0.05$), of which 556 genes were upregulated. There were 125 downregulated genes (Fig. 3A). Then, using GO/KEGG in conjunction with logFC, we conducted functional cluster analysis for these DEGs in order to better ascertain their functional roles. The findings showed that DEGs linked to LONP1 were engaged in the detoxification and metal ion stress response as well as molecular signal transmission (Fig. 3B).

Since LONP1 is an important mitochondrial protease, we first considered indicators related to mitochondrial function. Free radicals in living organisms can cause peroxidation of membrane lipids and lead to cross-linking polymerization of macromolecules such as proteins and nucleic acids, which is cytotoxic. Malondialdehyde (MDA) is an important metabolic product of oxygen free radicals (OFRs) *in vivo*. In this study, a small interfering RNA (siRNA) strategy was used to silence the expression of LONP1 in Huh7 cells (Fig. 3C–E), and the levels of MDA in the cells were significantly increased (Fig. 3F), which was due to the increase in lipid peroxides caused by the intensification of the ferroptosis process in the cells, suggesting that inhibiting LONP1 could promote ferroptosis. Thus, LONP1 is a negative regulator of ferroptosis. When LONP1 expression was knocked down and erastin-treated cells were added, the glutathione (GSH)/oxidized glutathione (GSSG) ratio increased (Fig. 3G), but LONP1 inhibition alone had no significant effect on the GSH/GSSG ratio. These findings suggest that the body's regulation of ferroptosis is more complicated when the cells are under severe oxidative stress. Mitochondrial function experiments indicated that knockdown of LONP1 led to a significant decrease in mitochondrial membrane potential (tetramethylrhodamine ethyl ester perchlorate (TMRE) fluorescence signal) (Fig. 3H), suggesting mitochondrial dysfunction.

According to the previous analysis of TCGA database—the function of LONP1 protein in response to copper stress and the correlation with detoxification of copper ion (Fig. 3B), we also speculated that LONP1 may be involved to cuproptosis. To explore the involvement of LONP1 in the regulation of cuproptosis (Fig. 3I). Further analysis of lentiviral stable LONP1-KD and LONP1-OE cell lines in this study found that inhibition of LONP1 expression could promote the upregulation of ACO2 protein in Huh7 cells, while overexpression of LONP1 could inhibit the expression of ACO2 (Fig. 3J). Meanwhile, histological analysis showed that the lower expression of LONP1 in liver cancer tissues accompanied by an increase in the level of ACO2 protein (Fig. 3K), confirming that the LONP1-ACO2 axis promotes the malignant progression of liver cancer by maintaining the stability of mitochondrial membrane potential and antagonizing ferroptose-dependent cell death.

3.4 Clinical Correlation Between LONP1 and HCC

To further verify the expression of the LONP1 and ACO2 proteins, 144 liver cancer tissue samples were subjected to immunohistochemical staining. The results revealed that the expression of LONP1 in cancer tissue was significantly greater than that in paracancerous tissue, while the expression of ACO2 was opposite (Fig. 4A). Moreover, the differential expression of these two proteins is correlated (Fig. 4B).

Accordingly, we distinguished liver cancer patients according to the median expression of LONP1 protein in liver cancer tissue chips (Table 2). Compared to patients with low LONP1 expression, HCC patients with high LONP1 expression had significantly shorter OS and disease-free survival (DFS), according to the KM curve, while the opposite was true for ACO2 (Fig. 4C). Accordingly, further univariate and multivariate Cox analyses suggested that LONP1 was an independent prognostic predic-

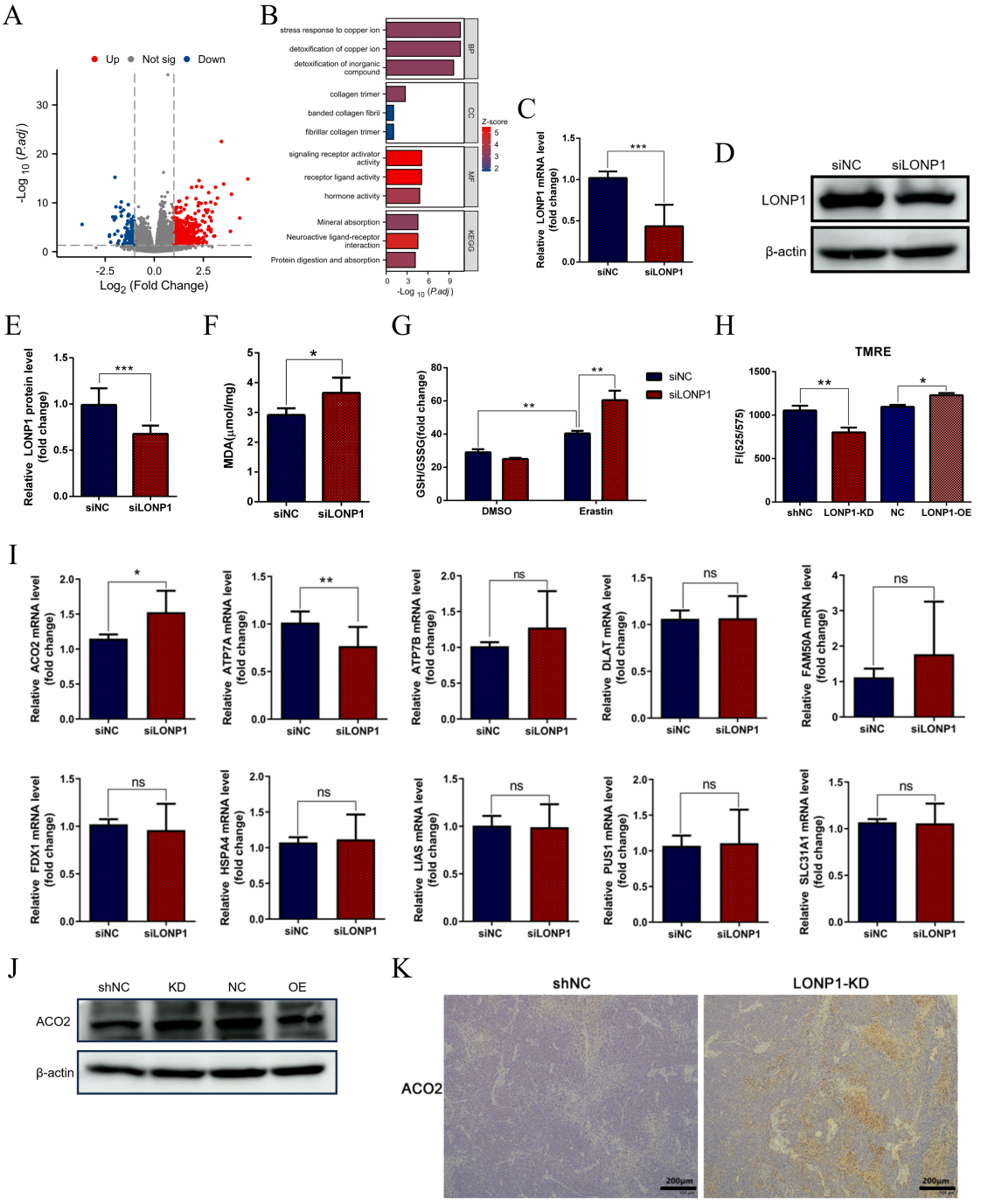

Fig. 3. Knocking down LONP1 expression promotes ferroptosis. (A) HCC-related single-gene difference analysis was performed on LONP1 RNAseq data from the TCGA database. (B) Functional cluster analysis of Gene Ontology/Kyoto Encyclopedia of Genes and Genomes (GO/KEGG) combined with logFC was performed for the DEGs in (A). (C) RT-qPCR detection of LONP1 expression by small interfering RNA (siRNA). (D) Western blot detection of LONP1 expression following small interfering RNA (siRNA), and representative images were selected. (E) Quantitative statistics of the data in (D). (F) Statistical analysis of the detected MDA levels. (G) The glutathione (GSH)/oxidized glutathione (GSSG) ratio measurement and statistical analysis. (H) The changes of mitochondrial membrane potential were detected by TMRE fluorescence signal. (I) RT-qPCR detection of mRNA expression levels of several cuproptosis related genes in Huh7 cell samples with LONP1 knockdown by siRNA. (J) Huh7 cells with stable knockdown or overexpression of LONP1were constructed, and the relative expression of ACO2 was detected via western blotting. The internal reference was beta-actin, and representative images were selected. (K) Hematoxylin-Eosinand Immunohistochemistry of Liver cancer subcutaneous tumors section. Scale bar = 200 μm. DEGs, differentially expressed genes; MDA, malondialdehyde; ACO2, aconitase 2; TMRE, tetramethylrhodamine ethyl ester perchlorate. *$p < 0.05$; **$p < 0.01$; ***$p < 0.001$; ns, not significant.

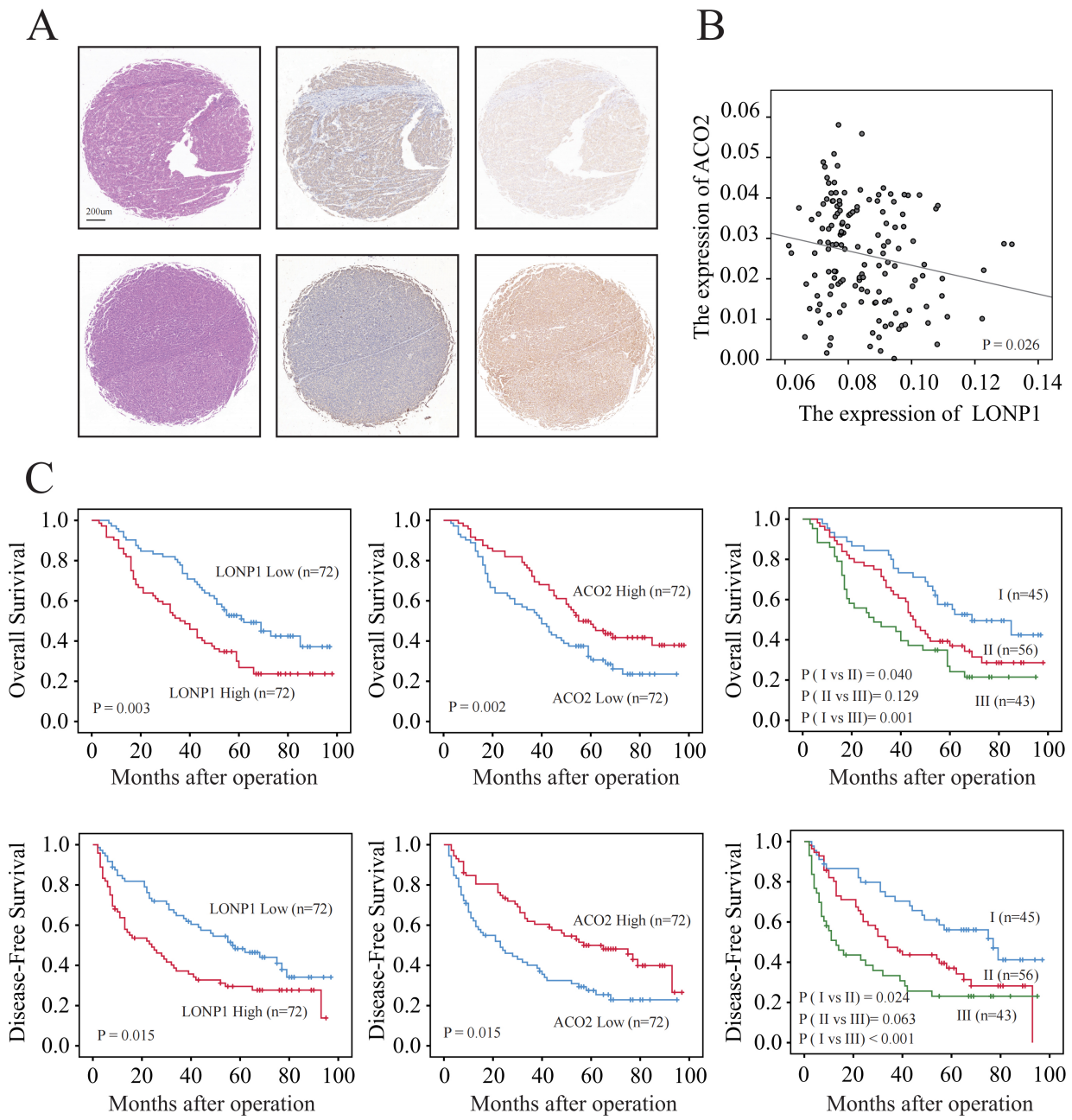

Fig. 4. Elevated protein level and prognostic value of LONP1. (A) Illustration of high and low LONP1 and ACO2 expression in liver cancer tissue chips detected by IHC. Scale bar = 200 μm. (B) Scatter plot of the correlation between LONP1 and ACO2 protein expression. (C) KM curve. The data used for the analysis were derived from the IHC analysis statistics of 144 liver cancer tissue chips.

tor of liver cancer (Table 3). Therefore, we confirmed that LONP1 is a liver cancer oncogene.

4. Discussion

HCC is the fourth leading cause of cancer-related death and continues to increase worldwide, representing a major challenge for global health care. The biological process of HCC is complex and involves a variety of factors, and regulation of liver cancer cell differentiation and angiogenesis [36]. However, owing to the insidious onset of HCC, most HCC patients are already in the advanced stage when diagnosed and can only receive systemic therapy [37]. Systemic antitumor therapy is the best treatment for patients with advanced liver cancer. With the approval of several new drugs for the treatment of advanced HCC and the establishment of checkpoint inhibitor-based therapy as the standard of care [38], the therapeutic landscape for advanced HCC is more diverse than ever before.

In this study, statistical analysis of RNAseq samples of the *LONP1* gene in the database revealed that the gene

Table 2. Relationship between LONP1 expression and HCC clinical features (n = 144).

Clinical characteristics	LONP1 expression		*p* value
	Low (n = 72)	High (n = 72)	
Sex (Female vs. Male)			0.085
Female	13	6	
Male	59	66	
Age, year (≤50 vs. >50)			0.045
≤50	28	40	
>50	44	32	
AFP, ng/mL (≤13.4 vs. >13.4)			0.003
≤13.4	35	18	
>13.4	37	54	
HBsAg (Negative vs. Positive)			0.479
Negative	9	12	
Positive	63	60	
Liver cirrhosis (Negative vs. Positive)			0.354
Negative	13	9	
Positive	59	63	
Tumor size, cm (≤5 vs. >5)			0.003
≤5 cm	47	29	
>5 cm	25	43	
Tumor number (Single vs. Multiple)			0.248
Single	57	51	
Multiple	15	21	
Tumor encapsulation (Complete vs. None)			0.074
Complete	54	44	
None	18	28	
Vascular invasion (Negative vs. Positive)			0.045
Negative	45	33	
Positive	27	39	
Tumor differentiation (I+II vs. III+IV)			1.000
I+II	46	46	
III+IV	26	26	
TNM stage (I vs. II+III)			0.001
I	40	21	
II+III	32	51	

LONP1, Lon protease 1; HCC, hepatocellular carcinoma; AFP, alpha fetoprotein; HBsAg, hepatitis B surface antigen; TNM, tumor node metastasis.

was differentially expressed in a variety of malignant tumors and their adjacent or normal tissues and was significantly highly expressed in HCC, suggesting that the protein encoded by the *LONP1* gene plays an important role in tumor occurrence and development. We subsequently analyzed the expression level of the LONP1 protein in the liver cancer microtissue chip, and the results were mutually confirmed with the RNA-seq data, indicating that LONP1 was significantly highly expressed in liver cancer. Finally, these results were also verified via RT-qPCR and IHC experiments. Additionally, the development of therapeutic strategies targeting LONP1 could potentially alleviate the clinical pathology in HCC patients. After identifying the significant correlation between LONP1 and the occurrence and development of liver cancer, we further explored the function and mechanism of this gene at the cellular and animal levels.

Given the high expression of LONP1 in HCC, we first investigated whether the proliferation and migration of HCC cells were affected by LONP1 expression. To support long-term functional studies, we adopted a lentivirus interference strategy to construct stable Huh7 cell lines with low knockdown and overexpression of LONP1. The results showed that knocking down LONP1 inhibited the proliferation and migration of Huh7 cells, whereas overexpressing LONP1 increased the proliferation and migration of Huh7 cells. We subsequently verified these findings at the animal level, and the results showed that the inhibition of LONP1 expression significantly inhibited the growth of Huh7 tumors *in vivo*. We found that LONP1 is a tumor-promoting

Table 3. Univariate and multivariate analyses of prognostic factors with OS and DFS in HCC (n = 144).

Variable	OS		DFS	
	HR (95% CI)	*p*	HR (95% CI)	*p*
Univariate analysis				
Sex (Female vs. Male)	1.435 (0.744–2.767)	0.281	1.427 (0.737–2.763)	0.291
Age, year (≤50 vs. >50)	0.745 (0.497–1.119)	0.156	0.707 (0.469–1.066)	0.098
AFP, ng/mL (≤13.4 vs. >13.4)	1.392 (0.91–2.13)	0.127	1.468 (0.952–2.263)	0.082
HBsAg (Negative vs. Positive)	1.363 (0.726–2.558)	0.335	1.14 (0.621–2.096)	0.672
Liver cirrhosis (No vs. Yes)	1.307 (0.727–2.351)	0.371	1.307 (0.724–2.36)	0.374
Tumor size, cm (≤5 vs. >5)	1.548 (1.031–2.323)	0.035	1.915 (1.268–2.893)	0.002
Tumor number (Single vs. Multiple)	1.962 (1.269–3.033)	0.002	2.078 (1.335–3.232)	0.001
Tumor encapsulation (Complete vs. None)	1.641 (1.078–2.499)	0.021	1.878 (1.231–2.865)	0.003
Vascular invasion (Negative vs. Positive)	1.872 (1.246–2.814)	0.003	1.836 (1.212–2.78)	0.004
Tumor differentiation (I+II vs. III+IV)	1.688 (1.118–2.548)	0.013	1.703 (1.123–2.584)	0.012
TNM stage (I vs. II+III)	3.159 (2.019–4.942)	0.000	2.72 (1.747–4.234)	0.000
LONP1 (Low vs. High)	1.855 (1.231–2.797)	0.003	1.748 (1.156–2.642)	0.008
Multivariate analysis				
Tumor size, cm (≤5 vs. >5)	1.367 (0.891–2.097)	0.152	1.828 (1.177–2.839)	0.007
Tumor number (Single vs. Multiple)	1.946 (1.252–3.025)	0.003	2.141 (1.361–3.367)	0.001
Tumor encapsulation (Complete vs. None)	1.102 (0.695–1.749)	0.679	1.217 (0.764–1.939)	0.409
Vascular invasion (Negative vs. Positive)	1.621 (1.034–2.542)	0.035	1.437 (0.911–2.268)	0.119
Tumor differentiation (I+II vs. III+IV)	1.841 (1.205–2.81)	0.005	1.772 (1.155–2.717)	0.009
LONP1 (Low vs. High)	1.712 (1.127–2.6)	0.012	1.601 (1.049–2.443)	0.029

OS, overall survival; DFS, disease-free survival; HR, hazard ratio; CI, confidence interval.

factor in HCC. These results are consistent with our previous findings and further elucidate the clinical value and significance of targeting LONP1.

This suggests that the aberrant expression of LONP1 in HCC may be associated with the ferroptosis process in tumor cells. Furthermore, LONP1 may interact with other mitochondrial proteins to regulate cell ferroptosis. Subsequently, we investigated the impact of the *LONP1* gene on the ferroptosis process. siRNA strategy was used in Huh7 cells to lower the expression of LONP1, and changes in the ferroptosis-related indicators GSH/GSSG ratio and MDA accumulation were detected. The results revealed that when LONP1 was silenced as a single factor, the MDA contents were increased in Huh7 cells, but the GSH/GSSG ratio remained unchanged. However, the GSH/GSSG ratio was significantly increased when erastin treatment was combined with LONP1 silencing, suggesting that the ability of LONP1 to promote ferroptosis was weakened when the cells were severely damaged. These experimental results are consistent with existing studies in the field of chronic kidney diseases, and inhibition of the *LONP1* gene can aggravate kidney injury and mitochondrial dysfunction [39].

In terms of the mechanism of action of LONP1, many studies have reported that LONP1 plays a role in protecting cell homeostasis by regulating mitochondrial function. LONP1 is a mitochondrial protease that is involved in the degradation of abnormal proteins in mitochondria due to oxidative damage or misfolding and is extremely important for maintaining the normal function of mitochondria [40,41]. LONP expression induced by LONP1 in the liver can counteract the silencing effect of mitochondrial transcription factor A (TFAM), thereby maintaining the copy number of mitochondrial DNA (mtDNA) and mitochondrial function [42]. The inhibition of mitochondrial LONP1 activity by specific siRNAs can affect liver function [43,44]. In addition, abnormalities in LONP1 are also associated with the development of other tumors [15], and are involved in cardiac stress [45]. As ACO2 is a mitochondrial protein, it plays a key role in TCA cycle, maintenance of iron homeostasis, oxidative stress defense, and integrity of mtDNA [46]. In this study, we found that knocking down LONP1 in Huh7 cells can promote the upregulated expression of ACO2. Correspondingly, the overexpression of LONP1 inhibited the expression of ACO2. ACO2 is a key mitochondrial protein involved in the TCA cycle, suggesting that LONP1 may influence mitochondrial function by modulating ACO2 expression, thereby regulating the proliferation and migration of liver cancer cells. Studies have shown that ACO2 affects the tumorigenicity of non-small cell lung cancer by regulating iron homeostasis [47]. ACO2 dysfunction can promote mitochondrial dysfunction, thus affecting the occurrence and development of different diseases [48]. In addition, we propose other hypotheses concerning the molecular mechanism of the cellular function and related signaling pathways of LONP1 [49–52]. GPX4 converts reduced GSH to GSSG, thereby

protecting cells against ferroptosis by limiting cytotoxic lipid peroxidation [53]. The GPX4 pathway is further regulated by amino acid antitransporters with xCT/SLC7A11 participation [54–56]. Importantly, the ferroptosis inducer erastin works by directly inhibiting the function of this heterodimer. In this study, the inhibition of LONP1 expression and erastin treatment resulted in an increased GSH/GSSG ratio and increased MDA accumulation, indicating that the pathway of GSH to GSSG transformation was blocked and that GPX4 may be inactivated. In other words, LONP1 may be involved in the regulation of ferroptosis via this pathway, thereby promoting cell proliferation, migration, and tumor formation. Based on relevant detection indicators, it is plausible that LONP1 exerts its effects through GPX4. It is important to note that no interactions between GPX4 and ACO2 have been reported in the literature. This mechanism remains underexplored and will be a key focus of our future studies. And we will enhance our investigation of mitochondrial function and elucidate the potential mechanisms underlying the LONP1/ACO2 axis in greater detail. LONP1 can also be used to predict the prognosis, immunotherapy response and sorafenib sensitivity of HCC patients [57]. p53, as a key tumor suppressor, plays a significant role in regulating apoptosis, autophagy and ferroptosis. Previous studies have shown that p53 can affect the ferroptosis process by regulating the expression of SLC7A11[27].

This study reveals a novel mechanism by which LONP1 inhibits ferroptosis in liver cancer by specifically degrading ACO2. This discovery expands our understanding of the carci9genic effect of LONP1 and shows similarities and differences with other types of cancer. Unlike the direct regulation of ferroptosis by LONP1 in this study, research in malignant tumors such as pancreatic cancer, breast cancer and ovarian cancer mostly emphasizes that LONP1 promotes tumor survival and proliferation by maintaining mitochondrial protein homeostasis, energy metabolism (such as stabilizing the key enzyme isocitrate dehydrogenase 2 (IDH2) of the TCA cycle) and resisting apoptosis (such as degrading pro-apoptotic factors). For instance, in glioblastoma, LONP1 has been reported to maintain mitochondrial genomic stability by eliminating oxidative damage proteins, but its association with the ferroptosis pathway has not been elaborated in depth. In colorectal cancer (though excluded but used as a comparison point) and lung cancer, the pro-cancer effect of LONP1 is often associated with antioxidant stress (such as regulating the nuclear factor erythroid 2-related factor 2 (NRF2) pathway) and metabolic reprogramming. Therefore, this study found that LONP1 directly alleviates ferroptosis by targeting and degrading ACO2. This not only provides a new perspective for the occurrence of liver cancer but also highlights the tissue or environmental specificity of LONP1's carcinogenic function—in liver cancer, its unique ability to counteract ferroptosis may constitute a key carcinogenic driving force. This is significantly different from the mode in which LONP1 mainly supports basal metabolism and anti-apoptosis in other cancers, suggesting the potential of tissue-specific therapeutic targeting strategies.

In our study, LONP1 alleviated ferroptosis by degrading ACO2, thereby promoting the occurrence of HCC. However, the role of LONP1 is not limited to intracellular metabolic regulation; its role in the tumor immune microenvironment is also worthy of attention. Furthermore, the mechanism by which lncRNAs regulate LONP1 in gastric cancer [16] suggests that there may be similar pathways associated with HCC. These lncRNAs may further affect the activity of immune cells in the HCC microenvironment by regulating the expression of LONP1. Therefore, future research should delve deeply into the specific role of LONP1 in immune regulation in HCC, so as to gain a more comprehensive understanding of its multiple mechanisms in the occurrence and development of hepatocellular carcinoma.

In this study, highly expressed LONP1 in HCC participated in the regulation of ferroptosis, promoted the proliferation and migration of Huh7 cells, and thus affected tumor formation. Silencing its expression in HCC may play an important role in providing a new way to stop the progression of clinical HCC. Validation using bioinformatics data and clinical tissue microarrays from our research group suggests that LONP1 may exert its oncogenic effects through ACO2. We hypothesize that LONP1, at normal expression levels, primarily functions to maintain mitochondrial function in normal liver tissue. However, in cancerous tissues with overexpressed LONP1, the excess LONP1 may dissociate from the mitochondria and regulate the expression of ACO2, thereby inhibiting ferroptosis in liver cancer cells. A limitation of this study is that we have not explored the molecular regulatory mechanisms between LONP1, ACO2, and GPX4. Due to time constraints, we regret that we are unable to present research findings on this aspect at this time. Additionally, the biological regulatory roles of LONP1 and ACO2 in normal liver tissue have not been fully investigated.

5. Conclusion

By preventing ferroptosis and cuproptosis through the breakdown of ACO2, LONP1 stimulates HCC migration and proliferation. LONP1 targeting may be a useful therapeutic approach to stop the formation of HCC.

Availability of Data and Materials

The datasets used or analyzed during the current study are available from the corresponding authors on reasonable request.

Author Contributions

YZ, LW: Designed the experiments, Performed the experiments; Collected and analyzed data; Wrote the paper. ZP, WM, TW: technique support. BW, ZY: Designed the

experiments and supervision. XL, EC: Designed the experiments, Supervision, and Funding acquisition. All authors contributed to editorial changes in the manuscript. All authors read and approved the final manuscript. All authors have participated sufficiently in the work and agreed to be accountable for all aspects of the work.

Ethics Approval and Consent to Participate

This retrospective study was approved by the Institutional Review Board of Peking University Shenzhen Hospital (Approval Number: [2022]No.(164)). Given the retrospective nature of the study and the use of de-identified patient data, the requirement for informed consent was waived by the IRB. The study was conducted in accordance with the ethical standards of the Declaration of Helsinki and its later Follow-up review (Approval Number: [2022]No.(164-Extension 1)). The animal study protocol was approved by the Institutional Review Board (or Ethics Committee) of Peking University Shenzhen Hospital (protocol code 2023-959) for studies involving animals. All animal experiments and operations strictly adhere to the experimental protocols approved by the Laboratory Animal Ethics Committee of Peking University Shenzhen Hospital, as well as national and international laboratory animal welfare guidelines. All experimental animals were euthanized by trained researchers proficient in the cervical dislocation method.

Acknowledgment

We would like to express our gratitude to all those who helped me during the writing of this manuscript, thanks to all the peer reviewers for their opinions and suggestions.

Funding

This work was supported by the National Natural Science Foundation of China (82303446), the Shenzhen High-level Hospital Construction Fund and Peking University Shenzhen Hospital Scientific Research Fund (KYQD2023303), GuangDong Basic and Applied Basic Research Foundation (2023A1515220200), Medical Scientific Research Foundation of Guangdong Province of China (A2024351) and the Science and Technology Development Fund Project of Shenzhen (JCYJ20190809095011463).

Conflict of Interest

The authors declare no conflict of interest.

References

[1] Llovet JM, Zucman-Rossi J, Pikarsky E, Sangro B, Schwartz M, Sherman M, *et al*. Hepatocellular carcinoma. Nature Reviews. Disease Primers. 2016; 2: 16018. https://doi.org/10.1038/nrdp.2016.18.

[2] Sung H, Ferlay J, Siegel RL, Laversanne M, Soerjomataram I, Jemal A, *et al*. Global Cancer Statistics 2020: GLOBOCAN Estimates of Incidence and Mortality Worldwide for 36 Cancers in 185 Countries. CA: a Cancer Journal for Clinicians. 2021; 71: 209–249. https://doi.org/10.3322/caac.21660.

[3] Li Y, Yu Y, Yang L, Wang R. Insights into the Role of Oxidative Stress in Hepatocellular Carcinoma Development. Frontiers in Bioscience (Landmark edition). 2023; 28: 286. https://doi.org/10.31083/j.fbl2811286.

[4] Pennisi G, Celsa C, Giammanco A, Spatola F, Petta S. The Burden of Hepatocellular Carcinoma in Non-Alcoholic Fatty Liver Disease: Screening Issue and Future Perspectives. International Journal of Molecular Sciences. 2019; 20: 5613. https://doi.org/10.3390/ijms20225613.

[5] Villanueva A, Hoshida Y, Battiston C, Tovar V, Sia D, Alsinet C, *et al*. Combining clinical, pathology, and gene expression data to predict recurrence of hepatocellular carcinoma. Gastroenterology. 2011; 140: 1501–12.e2. https://doi.org/10.1053/j.gastro.2011.02.006.

[6] Llovet JM, De Baere T, Kulik L, Haber PK, Greten TF, Meyer T, *et al*. Locoregional therapies in the era of molecular and immune treatments for hepatocellular carcinoma. Nature Reviews. Gastroenterology & Hepatology. 2021; 18: 293–313. https://doi.org/10.1038/s41575-020-00395-0.

[7] Bruix J, Llovet JM. Prognostic prediction and treatment strategy in hepatocellular carcinoma. Hepatology (Baltimore, Md.). 2002; 35: 519–524. https://doi.org/10.1053/jhep.2002.32089.

[8] Nagaraju GP, Dariya B, Kasa P, Peela S, El-Rayes BF. Epigenetics in hepatocellular carcinoma. Seminars in Cancer Biology. 2022; 86: 622–632. https://doi.org/10.1016/j.semcancer.2021.07.017.

[9] Chen E, He Y, Jiang J, Yi J, Zou Z, Song Q, *et al*. CDCA8 induced by NF-YA promotes hepatocellular carcinoma progression by regulating the MEK/ERK pathway. Experimental Hematology & Oncology. 2023; 12: 9. https://doi.org/10.1186/s40164-022-00366-y.

[10] Chen E, Zou Z, Wang R, Liu J, Peng Z, Gan Z, *et al*. Predictive value of a stemness-based classifier for prognosis and immunotherapy response of hepatocellular carcinoma based on bioinformatics and machine-learning strategies. Frontiers in Immunology. 2024; 15: 1244392. https://doi.org/10.3389/fimmu.2024.1244392.

[11] Bota DA, Davies KJ. Protein degradation in mitochondria: implications for oxidative stress, aging and disease: a novel etiological classification of mitochondrial proteolytic disorders. Mitochondrion. 2001; 1: 33–49. https://doi.org/10.1016/s1567-7249(01)00005-8.

[12] Bahat A, Perlberg S, Melamed-Book N, Isaac S, Eden A, Lauria I, *et al*. Transcriptional activation of LON Gene by a new form of mitochondrial stress: A role for the nuclear respiratory factor 2 in StAR overload response (SOR). Molecular and Cellular Endocrinology. 2015; 408: 62–72. https://doi.org/10.1016/j.mce.2015.02.022.

[13] Ngo JK, Pomatto LCD, Bota DA, Koop AL, Davies KJA. Impairment of lon-induced protection against the accumulation of oxidized proteins in senescent wi-38 fibroblasts. The Journals of Gerontology. Series A, Biological Sciences and Medical Sciences. 2011; 66: 1178–1185. https://doi.org/10.1093/gerona/glr145.

[14] Sepuri NBV, Angireddy R, Srinivasan S, Guha M, Spear J, Lu B, *et al*. Mitochondrial LON protease-dependent degradation of cytochrome c oxidase subunits under hypoxia and myocardial ischemia. Biochimica et Biophysica Acta. Bioenergetics. 2017; 1858: 519–528. https://doi.org/10.1016/j.bbabio.2017.04.003.

[15] Gibellini L, Losi L, De Biasi S, Nasi M, Lo Tartaro D, Pecorini S, *et al*. LonP1 Differently Modulates Mitochondrial Function and Bioenergetics of Primary Versus Metastatic Colon Cancer Cells. Frontiers in Oncology. 2018; 8: 254. https://doi.org/10.3389/fonc.2018.00254.

[16] Yao F, Zhan Y, Pu Z, Lu Y, Chen J, Deng J, *et al*. LncRNAs Target Ferroptosis-Related Genes and Impair Activation of $CD4^+$ T Cell in Gastric Cancer. Frontiers in Cell and Developmental Biology. 2021; 9: 797339. https://doi.org/10.3389/fcell.2021.797339.

[17] Luo B, Wang M, Hou N, Hu X, Jia G, Qin X, *et al*. ATP-Dependent Lon Protease Contributes to Helicobacter pylori-Induced Gastric Carcinogenesis. Neoplasia (New York, N.Y.). 2016; 18: 242–252. https://doi.org/10.1016/j.neo.2016.03.001.

[18] Wu J, Wang Y, Jiang R, Xue R, Yin X, Wu M, *et al*. Ferroptosis in liver disease: new insights into disease mechanisms. Cell Death Discovery. 2021; 7: 276. https://doi.org/10.1038/s41420-021-00660-4.

[19] Mo Y, Zou Z, Chen E. Targeting ferroptosis in hepatocellular carcinoma. Hepatology International. 2024; 18: 32–49. https://doi.org/10.1007/s12072-023-10593-y.

[20] Dixon SJ, Lemberg KM, Lamprecht MR, Skouta R, Zaitsev EM, Gleason CE, *et al*. Ferroptosis: an iron-dependent form of nonapoptotic cell death. Cell. 2012; 149: 1060–1072. https://doi.org/10.1016/j.cell.2012.03.042.

[21] Yang WS, SriRamaratnam R, Welsch ME, Shimada K, Skouta R, Viswanathan VS, *et al*. Regulation of ferroptotic cancer cell death by GPX4. Cell. 2014; 156: 317–331. https://doi.org/10.1016/j.cell.2013.12.010.

[22] Seiler A, Schneider M, Förster H, Roth S, Wirth EK, Culmsee C, *et al*. Glutathione peroxidase 4 senses and translates oxidative stress into 12/15-lipoxygenase dependent- and AIF-mediated cell death. Cell Metabolism. 2008; 8: 237–248. https://doi.org/10.1016/j.cmet.2008.07.005.

[23] Doll S, Proneth B, Tyurina YY, Panzilius E, Kobayashi S, Ingold I, *et al*. ACSL4 dictates ferroptosis sensitivity by shaping cellular lipid composition. Nature Chemical Biology. 2017; 13: 91–98. https://doi.org/10.1038/nchembio.2239.

[24] Zou Y, Palte MJ, Deik AA, Li H, Eaton JK, Wang W, *et al*. A GPX4-dependent cancer cell state underlies the clear-cell morphology and confers sensitivity to ferroptosis. Nature Communications. 2019; 10: 1617. https://doi.org/10.1038/s41467-019-09277-9.

[25] Wu J, Minikes AM, Gao M, Bian H, Li Y, Stockwell BR, *et al*. Intercellular interaction dictates cancer cell ferroptosis via NF2-YAP signalling. Nature. 2019; 572: 402–406. https://doi.org/10.1038/s41586-019-1426-6.

[26] Brown CW, Amante JJ, Goel HL, Mercurio AM. The $\alpha 6\beta 4$ integrin promotes resistance to ferroptosis. The Journal of Cell Biology. 2017; 216: 4287–4297. https://doi.org/10.1083/jcb.201701136.

[27] Wang SJ, Li D, Ou Y, Jiang L, Chen Y, Zhao Y, *et al*. Acetylation Is Crucial for p53-Mediated Ferroptosis and Tumor Suppression. Cell Reports. 2016; 17: 366–373. https://doi.org/10.1016/j.celrep.2016.09.022.

[28] Chu B, Kon N, Chen D, Li T, Liu T, Jiang L, *et al*. ALOX12 is required for p53-mediated tumour suppression through a distinct ferroptosis pathway. Nature Cell Biology. 2019; 21: 579–591. https://doi.org/10.1038/s41556-019-0305-6.

[29] Wenzel SE, Tyurina YY, Zhao J, St Croix CM, Dar HH, Mao G, *et al*. PEBP1 Wardens Ferroptosis by Enabling Lipoxygenase Generation of Lipid Death Signals. Cell. 2017; 171: 628–641.e26. https://doi.org/10.1016/j.cell.2017.09.044.

[30] Spiegel R, Pines O, Ta-Shma A, Burak E, Shaag A, Halvardson J, *et al*. Infantile cerebellar-retinal degeneration associated with a mutation in mitochondrial aconitase, ACO2. American Journal of Human Genetics. 2012; 90: 518–523. https://doi.org/10.1016/j.ajhg.2012.01.009.

[31] Zhu J, Xu F, Lai H, Yuan H, Li XY, Hu J, *et al*. ACO2 deficiency increases vulnerability to Parkinson's disease via dysregulating mitochondrial function and histone acetylation-mediated transcription of autophagy genes. Communications Biology. 2023; 6: 1201. https://doi.org/10.1038/s42003-023-05570-y.

[32] Sun LY, Lyu YY, Zhang HY, Shen Z, Lin GQ, Geng N, *et al*. Nuclear Receptor NR1D1 Regulates Abdominal Aortic Aneurysm Development by Targeting the Mitochondrial Tricarboxylic Acid Cycle Enzyme Aconitase-2. Circulation. 2022; 146: 1591–1609. https://doi.org/10.1161/CIRCULATIONAHA.121.057623.

[33] Palmieri EM, Gonzalez-Cotto M, Baseler WA, Davies LC, Ghesquière B, Maio N, *et al*. Nitric oxide orchestrates metabolic rewiring in M1 macrophages by targeting aconitase 2 and pyruvate dehydrogenase. Nature Communications. 2020; 11: 698. https://doi.org/10.1038/s41467-020-14433-7.

[34] Guo L, Hu C, Yao M, Han G. Mechanism of sorafenib resistance associated with ferroptosis in HCC. Frontiers in Pharmacology. 2023; 14: 1207496. https://doi.org/10.3389/fphar.2023.1207496.

[35] Pan F, Lin X, Hao L, Wang T, Song H, Wang R. The Critical Role of Ferroptosis in Hepatocellular Carcinoma. Frontiers in Cell and Developmental Biology. 2022; 10: 882571. https://doi.org/10.3389/fcell.2022.882571.

[36] Wang Y, Deng B. Hepatocellular carcinoma: molecular mechanism, targeted therapy, and biomarkers. Cancer Metastasis Reviews. 2023; 42: 629–652. https://doi.org/10.1007/s10555-023-10084-4.

[37] Yang C, Zhang H, Zhang L, Zhu AX, Bernards R, Qin W, *et al*. Evolving therapeutic landscape of advanced hepatocellular carcinoma. Nature Reviews. Gastroenterology & Hepatology. 2023; 20: 203–222. https://doi.org/10.1038/s41575-022-00704-9.

[38] Giraud J, Chalopin D, Blanc JF, Saleh M. Hepatocellular Carcinoma Immune Landscape and the Potential of Immunotherapies. Frontiers in Immunology. 2021; 12: 655697. https://doi.org/10.3389/fimmu.2021.655697.

[39] Wang H, Liu C, Zhao Y, Zhang W, Xu K, Li D, *et al*. Inhibition of LONP1 protects against erastin-induced ferroptosis in Pancreatic ductal adenocarcinoma PANC1 cells. Biochemical and Biophysical Research Communications. 2020; 522: 1063–1068. https://doi.org/10.1016/j.bbrc.2019.11.187.

[40] Matsushima Y, Goto YI, Kaguni LS. Mitochondrial Lon protease regulates mitochondrial DNA copy number and transcription by selective degradation of mitochondrial transcription factor A (TFAM). Proceedings of the National Academy of Sciences of the United States of America. 2010; 107: 18410–18415. https://doi.org/10.1073/pnas.1008924107.

[41] Lu B, Lee J, Nie X, Li M, Morozov YI, Venkatesh S, *et al*. Phosphorylation of human TFAM in mitochondria impairs DNA binding and promotes degradation by the AAA+ Lon protease. Molecular Cell. 2013; 49: 121–132. https://doi.org/10.1016/j.molcel.2012.10.023.

[42] Bonekamp NA, Jiang M, Motori E, Garcia Villegas R, Koolmeister C, Atanassov I, *et al*. High levels of TFAM repress mammalian mitochondrial DNA transcription in vivo. Life Science Alliance. 2021; 4: e202101034. https://doi.org/10.26508/lsa.202101034.

[43] Tian Q, Li T, Hou W, Zheng J, Schrum LW, Bonkovsky HL. Lon peptidase 1 (LONP1)-dependent breakdown of mitochondrial 5-aminolevulinic acid synthase protein by heme in human liver cells. The Journal of Biological Chemistry. 2011; 286: 26424–26430. https://doi.org/10.1074/jbc.M110.215772.

[44] Shan S, Liu Z, Wang S, Liu Z, Chao S, Zhang C, *et al*. Mitochondrial oxidative stress regulates LonP1-TDP-43 pathway and rises mitochondrial damage in carbon tetrachloride-induced liver fibrosis. Ecotoxicology and Environmental Safety. 2023; 264: 115409. https://doi.org/10.1016/j.ecoenv.2023.115409.

[45] Smyrnias I, Gray SP, Okonko DO, Sawyer G, Zoccarato A,

Catibog N, *et al*. Cardioprotective Effect of the Mitochondrial Unfolded Protein Response During Chronic Pressure Overload. Journal of the American College of Cardiology. 2019; 73: 1795–1806. https://doi.org/10.1016/j.jacc.2018.12.087.

[46] Rouault TA, Tong WH. Iron-sulphur cluster biogenesis and mitochondrial iron homeostasis. Nature Reviews. Molecular Cell Biology. 2005; 6: 345–351. https://doi.org/10.1038/nrm1620.

[47] Mirhadi S, Zhang W, Pham NA, Karimzadeh F, Pintilie M, Tong J, *et al*. Mitochondrial Aconitase ACO2 Links Iron Homeostasis with Tumorigenicity in Non-Small Cell Lung Cancer. Molecular Cancer Research: MCR. 2023; 21: 36–50. https://doi.org/10.1158/1541-7786.MCR-22-0163.

[48] Neumann MAC, Grossmann D, Schimpf-Linzenbold S, Dayan D, Stingl K, Ben-Menachem R, *et al*. Haploinsufficiency due to a novel ACO2 deletion causes mitochondrial dysfunction in fibroblasts from a patient with dominant optic nerve atrophy. Scientific Reports. 2020; 10: 16736. https://doi.org/10.1038/s41598-020-73557-4.

[49] Huo S, Wang Q, Shi W, Peng L, Jiang Y, Zhu M, *et al*. ATF3/SPI1/SLC31A1 Signaling Promotes Cuproptosis Induced by Advanced Glycosylation End Products in Diabetic Myocardial Injury. International Journal of Molecular Sciences. 2023; 24: 1667. https://doi.org/10.3390/ijms24021667.

[50] You X, Tian J, Zhang H, Guo Y, Yang J, Zhu C, *et al*. Loss of mitochondrial aconitase promotes colorectal cancer progression via SCD1-mediated lipid remodeling. Molecular Metabolism. 2021; 48: 101203. https://doi.org/10.1016/j.molmet.2021.101203.

[51] Sawant Dessai A, Dominguez MP, Chen UI, Hasper J, Prechtl C, Yu C, *et al*. Transcriptional Repression of SIRT3 Potentiates Mitochondrial Aconitase Activation to Drive Aggressive Prostate Cancer to the Bone. Cancer Research. 2021; 81: 50–63. https://doi.org/10.1158/0008-5472.CAN-20-1708.

[52] Chen Y, Cai GH, Xia B, Wang X, Zhang CC, Xie BC, *et al*. Mitochondrial aconitase controls adipogenesis through mediation of cellular ATP production. FASEB Journal: Official Publication of the Federation of American Societies for Experimental Biology. 2020; 34: 6688–6702. https://doi.org/10.1096/fj.201903224RR.

[53] Zhang Y, Swanda RV, Nie L, Liu X, Wang C, Lee H, *et al*. mTORC1 couples cyst(e)ine availability with GPX4 protein synthesis and ferroptosis regulation. Nature Communications. 2021; 12: 1589. https://doi.org/10.1038/s41467-021-21841-w.

[54] Yan R, Xie E, Li Y, Li J, Zhang Y, Chi X, *et al*. The structure of erastin-bound xCT-4F2hc complex reveals molecular mechanisms underlying erastin-induced ferroptosis. Cell Research. 2022; 32: 687–690. https://doi.org/10.1038/s41422-022-00642-w.

[55] Liu X, Zhuang L, Gan B. Disulfidptosis: disulfide stress-induced cell death. Trends in Cell Biology. 2024; 34: 327–337. https://doi.org/10.1016/j.tcb.2023.07.009.

[56] Koppula P, Zhuang L, Gan B. Cystine transporter SLC7A11/xCT in cancer: ferroptosis, nutrient dependency, and cancer therapy. Protein & Cell. 2021; 12: 599–620. https://doi.org/10.1007/s13238-020-00789-5.

[57] Zhang S, Guo H, Wang H, Liu X, Wang M, Liu X, *et al*. A novel mitochondrial unfolded protein response-related risk signature to predict prognosis, immunotherapy and sorafenib sensitivity in hepatocellular carcinoma. Apoptosis: an International Journal on Programmed Cell Death. 2024; 29: 768–784. https://doi.org/10.1007/s10495-024-01945-6.